



## What happens to heat transmission and pressure loss in a rectangular channel with semi-circular ribs when the ribs are spaced apart is of interest.

G SHIVA KUMAR 1, BANTU SAILESH 2,

ASSOCIATE PROFESSOR 2, ASSISTANT PROFESSOR 1,

[Mail ID: shivakumargaini@gmail.com](mailto:shivakumargaini@gmail.com), [Mail ID: sailesh.bantu04@gmail.com](mailto:salesh.bantu04@gmail.com)

Dept.: Mechanical

Pallavi Engineering College,

Kuntloor(V), Hayathnagar(M), Hyderabad, R.R. Dist. -501505.

### ABSTRACT

However, the effectiveness of ribs for improved heat transmission is highly dependent on their geometrical details and the prevailing flow conditions. This experiment investigates the effect of rib spacing by examining semi-circular ribs spaced at 8, 10, and 12 rib spacing ratios down the bottom of a rectangular channel. The channel blockage ratio ( $e/D_h$ ) was 0.151, and the Reynolds number ranged from 10,000 to 29,000. More friction is discovered; however, the findings reveal that semi-circular ribs work better than plain plates. There is a 39% increase in average heat transmission for a semi-circular rib with a rib spacing of 50 mm ( $P/e = 10$ ) compared to rib spacings of 40 and 60 mm ( $P/e = 8$  and 12), respectively. On average, friction losses were found to be 10% higher for a rib spacing ratio of 8 compared to a ratio of 10 or 12. When compared to alternative arrangements, a semi-circular rib with a spacing ratio of 8 provides the worst thermal performance.

Keywords:

Semi-circular ribs, increased heat conduction, rib spacing, a square cross section.

### INTRODUCTION

Gas turbine engines, which must run at the highest possible input temperature in order to maximize efficiency and output, are just one example of a field in which cutting-edge methods are being used to move closer to the ideal of maximum efficiency. The blade material could not withstand the high inflow temperature; thus, cooling is required to prolong the blade's useful life. Pin fin cooling, rib turbulators, dimple, protrusions, etc. are all examples of internal cooling techniques. Ribs are often favoured for cooling, and rib turbulators' efficacy is affected by a number of variables such as rib angle, blockage ratio, pitch ratio, rib shape, inclination of rib, and whether or not the ribs are stationary or spinning. Many studies on rib turbulators, which are used to increase heat transmission, have been published during the last few decades. Friction was shown to be greater than the heat transfer coefficient in a study by Luca Baggett a, who looked at a rib design with 45-degree angles and crossing ribs (Luca Baggett a et al. 2018). After analysing data from a thermal liquid crystal sheet, Kaewchoothong found that the

Nusselt number for 600, 450 angled ribs, and 600 V-shaped ribs was 20-30% higher than that of 900 angled ribs (Kaewchoothong et al. 2017). Reynolds number 80,000 was used in Liu's study of truncation ribs, and it was shown that these ribs decreased friction without affecting the heat transfer rate (Jian Liu et al. 2018). While others looked at numerical methods. At Reynolds numbers between 5000 and 50,000, Moon conducted a numerical study of sixteen different rib configurations. Utilizing the Reynolds stress model, it was determined that the boot-shaped rib provided the best performance (Mi-Ae Moon et al. 2014). Zheng uses simulation to determine the impact of rib configurations on the thermal performance of V-type and parallel ribs, and the results revealed that the V-type ribs performed better than the P-type ribs (Zheng et al. 2016). Shukla displayed 900 ribs, thick and thin, joined in a continuous V. It has been shown that the performance of thin ribs is enhanced by thick ribs, and that the optimum ratio of rib spacing to rib thickness is 10.

Nomenclature		
Symbol	Description	Units
$A$	rectangular duct cross section area	$m^2$
$h$	heat transfer coefficient	$W/m^2K$
$D_h$	Rect. duct hydraulic diameter	m
$W$	Width of rect. duct	m
$H$	height of rect. duct	m
$L$	Test section length	m
$p$	Rib pitch	m
$e$	Rib height	m

$\dot{m}$	Air mass flow rate	kg/s
$AR$	Channel aspect ratio (W/H)	
$p/\epsilon$	Ratio of rib pitch to rib height	
$Q_{net}$	Net Heat gain	W
$T_i$	Inlet temperature of air	$0^\circ\text{C}$ or K
$T_o$	outlet temperature of air	$0^\circ\text{C}$ or K
<b>Dimensionless number</b>		
$Re$	Reynolds number	
$Nu$	Nusselt number	
$Nu_s$	smooth duct Nusselt number	
$f$	Friction factor	
$f_o$	Friction factor for smooth duct	

and measured with an orifice plate assembly. To lessen the amount of heat that was lost by conduction, a rectangular channel fashioned from Bakelite was set up between the input and the outlet. The rectangular channel's length was 540 mm, while its hydraulic diameter ( $D_h$ ) was 30 mm. As a means of mitigating the negative impacts of flow termination, a base plate and heater were installed in the test portion of a rectangular channel, and an exit section with a length more than six times the hydraulic dia. of channel ( $D_h$ ) was connected there. Orifice plate and blower, as shown in an authentic image (Fig. 2).

## EXPERIMENTATION

Center for Experimental Research The experimental setup is planned, built, and checked before any data can be collected. Fig.1 is a schematic of the experimental setup, which comprises of a centrifugal blower, developing section, orifice plate with U tube manometer, intake section, rectangle channel with test section, exit section, k-type thermocouples, and data collecting system.

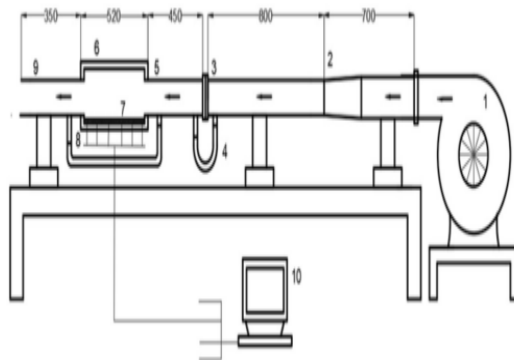


Figure 1. Schematic of experimental test facility.

- |   |                        |                             |
|---|------------------------|-----------------------------|
| 1-blower,                               | 5- Inlet section       | 8- Thermo-couples           |
| 2- developing section                   | 6- Rectangular channel | 9- Exit section             |
| 3 & 4- orifice plate & U tube manometer | 7- Test section        | 10- data acquisition system |

In the experimental set-up, a developing section came after the blower; its entire length was 1500 mm, and it was maintained longer than that to guarantee completely developed flow and regularize the flow. A long input portion, more than ten times the hydraulic dia. of channel ( $D_h$ ), follows the developing section, when the flow once again becomes uniform and regularized. The air mass flow rate was adjusted using a dimmer-stat

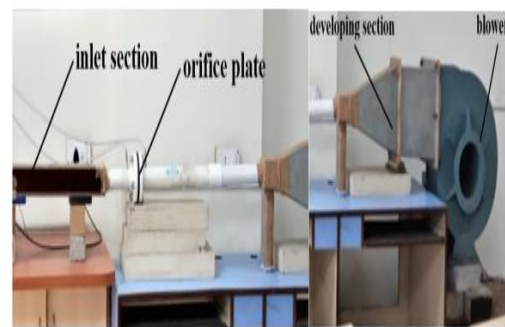


Figure .2There are pictures of the experimental setup. A micro manometer was attached to the entrance and exit of the test plate to measure the pressure drop along the rectangular channel. Two thermocouples, one on each end of the duct's entrance and departure, are hardwired to a data logger to record the incoming and outgoing air temperatures. Copper constant K-type thermocouples are used to detect temperatures, and there are twelve of them mounted on the surface of the test plate. The flat plate heater, 300 mm x 50 mm in size, was positioned between the test plate and the base plate to provide the uniform heat flux. All experimental equipment used in this study were calibrated by a NABL-accredited laboratory, and the heat input was controlled using a dimmer-stat. All data were first obtained over a period of 2–3 hours at steady state. Various Rib and Section Tests Aluminium was utilized for the test section, and the thickness and length of the test plate were 10 mm and 540 mm, respectively.

Thermal glue was used to adhere the semi-circular rib to the testing plate. We used nuts and bolts to securely fix the test plate, the heater, and the supporting plate into a rectangular channel. The insulating material is applied to the bottom of the heater and the walls to decrease heat loss. Structural arrangements of the ribs. Bonding

material is used to adhere the ribs to the sample section. Aluminium tubing with a diameter of 75 millimeters is used to create semi-circular ribs. To create round ribs, an aluminium pipe must first be hollowed out using a boring tool and its outside diameter must be properly sized using a lathe machine. Both the height and breadth of the rib are measured to be 5 mm. Rib pitch to rib height (P/e) = 8, 10, and 12 and the ratio of rib height to hydraulic dia. (Dh/e) = 0.156. The test plate and rectangular channel are shown in a real-life snapshot in Fig. 3.



Figure 3. a) rectangular duct with test section assembly (10 ribs and 12 ribs).



Figure 4. b) Semi-circular rib (P/e = 10 & 8).

Structure of the ribs. For this purpose, three ribbed channels with varying rib spacing have been made. The present investigation focuses on a first group of semi-circular ribs with a rib spacing ratio (P/e) = 8 and a distance of 40 mm between adjacent ribs. The same ribs are examined in a second set with a pitch-to-height ratio (P/e) of 10, resulting in a 50 mm gap between ribs; in a third set, the P/e is maintained at 12 for a 60 mm gap between ribs. The ribs were positioned on the channel bottom at an aspect ratio of 4:1, and the Reynolds number ranged from 10,000 to 29,000.

### CONSOLIDATION OF INFORMATION AND FAILURE ANALYSIS

Several metrics, including the friction factor, the Nusselt number, and the thermal performance, may be derived from the channel's recorded temperature and pressure data. Equation was used to get the heat transfer coefficient (ha) (1):

$$Q_{net} = ha A (T_s - T_b)$$

$$h = \frac{Q_{net}}{A(T_s - T_b)}$$

$$T_s = \frac{T_1 + T_2 + \dots + T_{12}}{12}, \quad T_b = \frac{T_{air\ in} + T_{air\ out}}{2}$$

where  $T_s$  is the typical surface temperature of the test plate and  $T_b$  is the typical temperature of the air around it. The maximum heat loss from the test section was determined to be less than 12% after taking into consideration heat losses from the test plate (conduction, convection). Using the formula (2), we were able to get the Nusselt number as follows:  $h$  = average heat transfer coefficient,  $D_h$  = hydraulic diameter of channel,  $A$  = cross section area of channel, and  $p$  = perimeter of channel:

$$Nu = \frac{h D_h}{k}$$

$$D_h = \frac{4 A}{p}$$

Nusselt number of plain plates was verified by using Dittus-Boelter correlation. To express the Nusselt number as a ratio, we have

$$Nu/Nu_0 = (h D_h / k) / (0.023 Re^{0.8} Pr^{0.4})$$

Frictional Losses. The friction factor was estimated by monitoring pressure drop along the test channel and compute using equation (4):

$$\Delta P = f L \rho V^2_{avg} / 2 D$$

$$f = (P_i - P_e) / [(4(L / D_h) (1/2 \rho V^2))]$$

By using the friction factor of a smooth plate, a frictional factor ratio may be determined. Values for the friction factor between a smooth plate and a rough surface are verified using the Blasius correlation.

$$f / f_0 = f / (0.079 Re^{-1/4})$$

Conductivity of Heat. Using the Nusselt number ratio (Nu/Nu<sub>0</sub>) and the frictional factor ratio (f/of), the thermal hydraulic performance was determined. Rib configuration performance ( ) was measured using equation (6).

$$\eta = (Nu/Nu_0) / (f/f_0)^{1/3}$$

## A Look at the Mistakes

Uncertainty analysis was performed using the Kline and McClintock (1953) approach, and it was determined that, in all instances, the computed uncertainty in the temperature measurement was less than 10. Approximately 8-11% of the experimental data were accounted for by the average uncertainty in the Nusselt number. While uncertainty led to greater heat loss at low Reynold's numbers, this effect was mitigated by increasing flow velocities. A total error of around 7–10% of the experimental values was observed in the friction factor.

In a Streamlined Duct, Heat Transfer Occurs Results from a correlation analysis are used to verify the accuracy of the smooth duct experiments. Comparison of the Nusselt number obtained experimentally with the value obtained from the Dittus-Boelter correlation (7) for the plain duct is shown in Fig. The experimental and correlational Nusselt numbers were shown to have a better relationship, with a maximum of 13% difference. The friction factor calculated from the modified Blasius equation (8) for a simple duct agrees with the experimental measurement. Meanwhile, as shown in Fig. (5), the observed largest 10% discrepancy between the theoretical and actual value of friction factor for a smooth duct coincides well with Blasius' correlation.

$$Nu_0 = 0.023 Re^{0.8} Pr^{0.4}$$

$$f_0 = 0.079 Re^{-1/4}$$

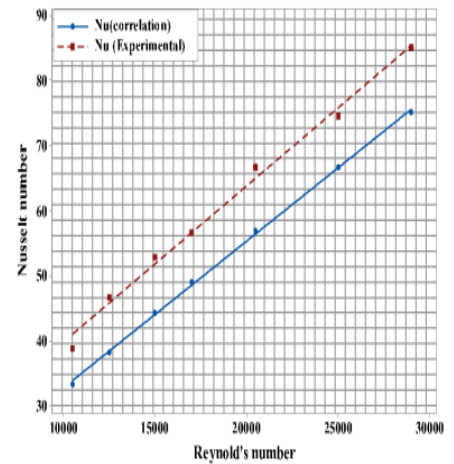


Figure 4. Comparison of smooth duct results of Nusselt number with correlation.

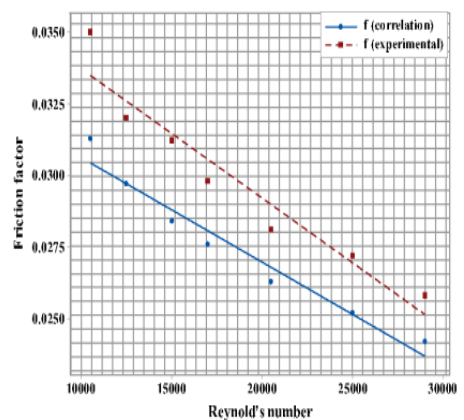


Figure 5. Comparison of smooth duct results with correlation

## RESULTS AND DISCUSSION

In this article, we show and analyse the Nusselt number and friction factor of all tested configurations from a Reynolds number of 10,000 to 29,000, respectively. Finding the best rib spacing for a semi-circular rib has required analysis and comparison of the outcomes of various designs.

### Ribbed duct heat transfer

Figure displays the computed Nusselt number of semi-circular ribs at different rib spacings based on the experimental results (6). With an increase in Reynolds number, the Nusselt number follows suit and exhibits an upward trend for all channels. The graph also shows that the semi-circular rib outperforms the plain plate by as much as 130% in

terms of heat transmission. Ribs applied to a surface improve heat transfer by increasing the area available for heat transfer and by increasing the spacing of rib turbulators on the flow boundary layer; however, the ribs also cause a pressure drop owing to the barrier they introduce. More surface area is exposed to air in front of semi-circular ribs because of their curvature, while less surface area is available for heat transmission in back. The fluid recirculation zone with low turbulent kinetic energy and velocity emerges behind the ribs in the case of semi-circular ribs, while high turbulent kinetic energy appears in the region between two adjacent ribs and in front of the ribs. Figure also shows that for semi-circular ribs, the best performance was achieved with a pitch-to-height ratio ( $P/e$ ) of 10, followed by  $P/e = 8$  and 12, at all Reynolds's numbers.

At a rib pitch ratio of 8 ( $P/e=40$  mm), the heat transfer rate is lowered because the flow cannot reattach itself to the rib wall as quickly due of the sluggish dropping of the rib pitch and the lack of flow reattachment events. Because the boundary layer grows later at reattachment points and also because the reattachment point at the wall was reached, and a boundary layer begins to develop early, and the subsequent rib comes across, the heat transfer rate is reduced at a rib pitch ratio of  $P/e = 12$ , but greater than 40 mm rib spacing. The separation vortex and reattachment effects on convective heat transmission are less, however, as rib spacing increases.

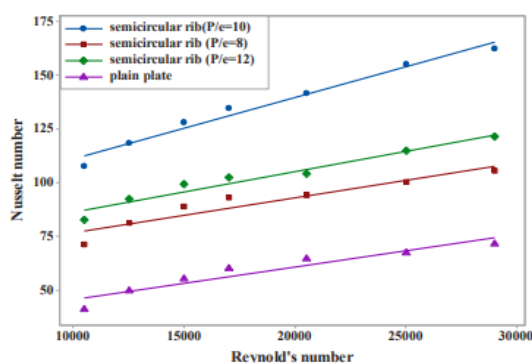


Figure 6. Reynold's number vs. Nusselt number for semi-circular rib.

When the rib pitch was set to 50 mm ( $P/e=10$ ), it was found that the heat transfer was the maximum. This is because the flow does reattach near the next rib, and the flow separation vortex and reattachment to the rib wall both play vital roles in enhancing the transfer. Furthermore, the flow

forcefully reattaches to the ribbed wall and then swiftly detaches again, as seen in the distinct separation zone and reattachment region between ribs. Secondary flow disrupts boundary layer formation on the side wall due to the enhanced surface heat transfer in the case of 50 mm separation, and efficient mixing between the mainstream and fluids was seen along the sides.

## Losses Due to Friction

Ribs improve heat transmission but increase pressure drop, and in general, ribs with rounded edges have less friction than ribs with sharp ones. In Fig. 1 we see the friction factor for the semi-circular rib channel (7). Since the initial resistance to flow is large, the retardation to flow decreases as the velocity increases, hence the friction factor decreases as the Reynolds number grows. Because the rib's enormous curvature generates more turbulence and the roughness component slows the flow and provides extra pressure drop, the rib's friction factor is higher than that of the plain plate. More friction is lost by the semi-circular rib than by the plain plate on average, and the semi-circular rib with a rib pitch ratio ( $P/e$ ) of 8 had the most friction loss of the configurations evaluated. More retardation and disturbance were introduced into the test plate at a rib pitch of 40 mm ( $P/e=8$ ), which reduced the space between adjacent ribs and increased the number of ribs on the plate, both of which contributed to an increase in friction. Thicker boundary layers between the two ribs contributed to the increased form drag we observed. With a rib pitch of 60 mm ( $P/e =12$ ), we discovered less friction than in any of the other studied instances. This is because the number of ribs on the test plate is decreased, and the space between two ribs is increased, since the separation zones between them are smaller. The channel provides medium friction at a rib pitch of 50 mm ( $P/e =10$ ), which corresponds to a rib spacing of between 40 and 60 mm; in this instance, the flow turbulence is moderate since the optimal distance is maintained between successive ribs.

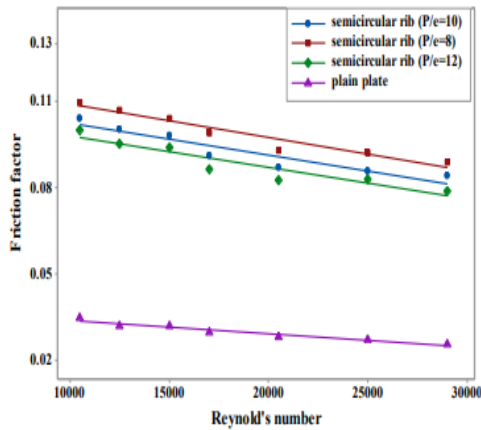


Figure 7. Reynold's number vs Friction factor for semi-circular rib.

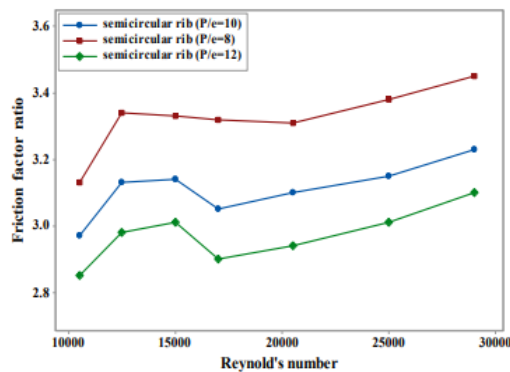


Figure 8. Variation of friction factor ratio against Reynold's number.

Fig. (8) displays the ratio of the friction factor for semi-circular ribs. Since the viscous sublayer is eliminated as the Reynolds number increases, and since the thickness of the boundary layer decreases as the Reynolds no. increases, the fluid velocities in the boundary layer increase, the friction factor ratio decreases from 10000 to 15000, but increases from 25000 onwards. The friction of a semi-circular rib with a pitch ratio of ( $P/e = 8$ ) is greater than that of a rib with a pitch ratio of ( $P/e = 10$ ) or ( $P/e = 12$ ). Lower friction was observed between semi-circular ribs with a 60 mm ( $P/e = 12$ ) spacing compared to ribs with a 40 mm ( $P/e = 6$ ) or 50 mm ( $P/e = 12$ ) spacing, likely because the larger the gap between ribs, the smaller the retardation to flow.

### Standardized Correlations of Experimental Measurements

The present findings were generalized using the least squares approach, and correlations were found between the Nusselt number ratio and the friction factor ratio in terms of the rib spacing ratio ( $P/e$ ) and the Reynolds number for the semi-circular rib with varying rib spacing configurations. To approximate the heat transfer improvement of ribbed surfaces, the thermal efficiency index criteria was used. Experimental findings were generalized using the semi-circular rib correlations given by Alfarawi et al. (2017). Summarized below are all the relevant associations, which hold true for ( $P/e$ ) values between 8 and 12 and Reynolds numbers between 10000 and 29000 in the context of the semi-circular rib duct. We utilized a ratio correlation (9) to analyse the Nusselt number and found that the experimental findings and the correlation results differed by no more than 13%.

$$Nu/Nus = 10.07 Re^{-0.164} [P/e]^{-0.0595}$$

Like with the friction factor ratio, correlation (10) was used to identify an allowable range of +/- 10%, and thermal performance or efficiency index equation (11) was utilized to obtain an allowable range of +/- 9.65%.

$$f/fo = 9.33 Re^{-0.041} [P/e]^{-0.28}$$

$$\eta_i = 4.73 Re^{-0.15} [P/e]^{0.034}$$

### Verification of Results from Ribbed Duct Utilizing Computational Fluid Dynamics

Numerical findings verify the semi-circular rib experiments, and STAR CCM version 2019 was utilized to do the simulations. The research validates the turbulence model's findings by comparing them to those from earlier papers, and the realizable k- turbulence model was chosen for the investigation. High turbulent kinetic energy appears in the center area between two neighbouring ribs and in front of the ribs, as seen by the top and side wall velocity contours of the semi-circular rib in Figure 9.

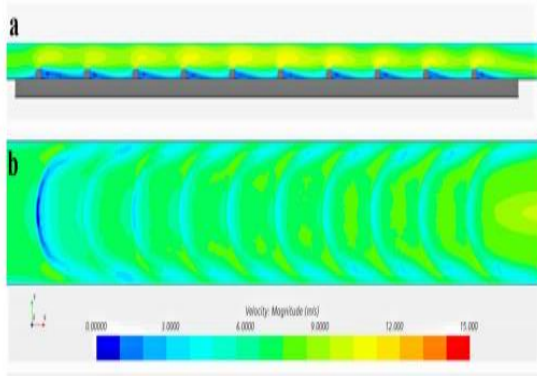


Figure 9. Side and top velocity contours of semi-circular rib.

In both the experiment and the simulation, the highest performance was shown for a semi-circular rib with a pitch ratio of 10 ( $P/e=10$ ). Semi-circular rib ( $P/e = 10$ ) experimental and numerical findings exhibit variance (Fig. 10 and 11). As can be seen in Fig., there is reduced scatter between the numerical and experimental data, and the numerical and experimental variances in the Nusselt number and friction factor values are less than 12%.

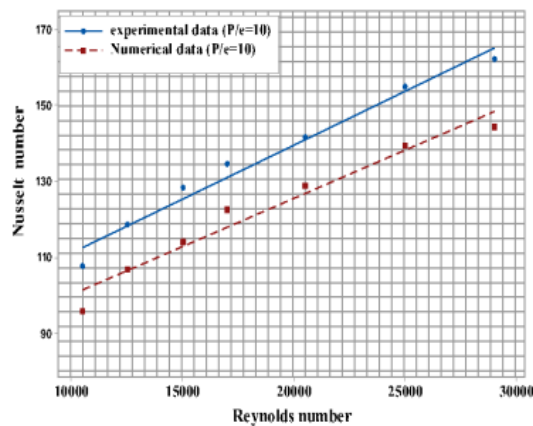


Figure 10. Variation of expt. and numerical results of Nusselt number.

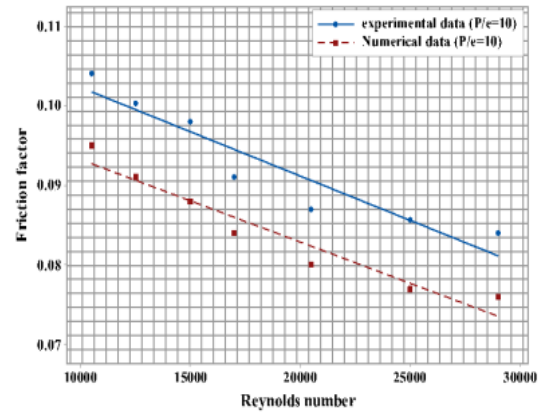


Figure 11. Variation of expt. and numerical results of friction factor.

### In terms of thermal efficiency, the phrase "performance" (T.P.)

Frictional losses are combined with Nusselt values for thermal performance evaluation. The thermal performance of all combinations is shown in Fig. (12). In terms of thermal efficiency, the semi-circular rib with a pitch spacing ratio ( $P/e$ ) of 10 was superior to all other layouts. When compared to the other rib spacing situations, the semi-circular rib with  $P/e = 10$  exhibits greater heat transfer enhancement and lower frictional losses. Lowest thermal performance was achieved by a semi-circular rib with a pitch ratio ( $P/e$ ) of 8.

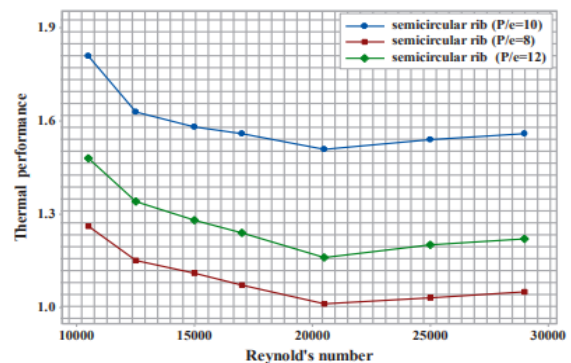


Figure 12. Reynold's number vs thermal performance.

### CONCLUSION

Experiments were conducted to examine the heat transfer and flow friction characteristics of a rectangular duct with three rib spacings ( $P/e = 8, 10, 12$ ).

**These inferences are drawn from the experimental findings:**



- The semi-circular rib outperformed the simple duct, increasing heat transmission by up to 130%. When comparing rib spacing ratios of 8, 10, and 12, it was shown that the semi-circular rib with a pitch to height ratio (P/e) of 10 had the maximum thermal performance, improving heat transmission by an average of 40%.
- The semi-circular rib with a pitch to height ratio (P/e) of 8 was found to have the maximum friction, followed by the semi-circular ribs with a P/e of 10 and 12. This is contrasted to the plain plate, where friction was on average 100% lower.
- The least thermal performance may be found in a semi-circular rib with a pitch to height ratio (P/e) of 8.

## REFERENCES

- [1] Luca Baggett a, Francesca Stata and Giovanni Tanda.2018. A Possible Strategy for the Performance Enhancement of Turbine Blade Internal Cooling with Inclined Ribs. Taylor & Francis, *heat transfer Engineering*, DOI: 10.1080/01457632.2017.1421305.
- [2] Mattaponi Kaewchoothong, Kittinan Maliwan, Kenichiro Takeishi and Chanut Nuntadusit. 2017. Effect of inclined ribs on heat transfer coefficient in stationary square channel. *Theoretical and Applied Mechanics Letters*, 7: 344-350.
- [3] Jian Liu, Safeer Hussain, Jinsheng Wang, Lei Wang, Gongnan Xia and Bengt Sundén. 2018. Heat Transfer enhancement and turbulent flow in a high aspect ratio channel (4:1) with ribs of various truncation types and arrangements. *International Journal of Thermal Sciences*, 123: 99-116.
- [4] Mi-Ae Moon, Min-Jung Park & Kwang-Yong Kim.2014. Evaluation of heat transfer performances of various rib shapes. *International Journal of Heat and Mass Transfer*, 71:275- 284.
- [5] Niaben Zheng, Peng Liu, Feng Shan, Zhichun Liu and Wei Liu. 2016. Effects of Rib arrangements on the flow pattern and Heat transfer in an internally Ribbed heat exchanger tube. *International Journal of Thermal Sciences*, 101:93-105.
- [6] Anuj K Shukla and Anupam Dewan. 2016. Computational study on effects of rib height and thickness on heat transfer Enhancement in a rib roughened square channel. *Sadhana, Indian Academy of Sciences*, 41(6):667- 678.
- [7] Goninan Xia, Jian Liu, Phillip M. Ligrani and Bengt Sundén.2014. Flow structure and heat transfer in a square passage with offset mid-truncated ribs. *International Journal of Heat and Mass Transfer*: 71, 44–56.
- [8] Wandong Bai, Wei Chen, Li Yang and Minking K. Chyu.2019. Numerical investigation on heat transfer and pressure drops of pin-fin array under the influence of rib turbulators induced vortices. *International Journal of Heat and Mass Transfer*: 129, 735–745.
- [9] Giovanni Tanda. 2011. Effect of rib spacing on heat transfer and friction in a rectangular channel with 450 angled rib Turbulators on one/two walls. *International Journal of Heat and Mass Transfer*, 54:1081- 1090.
- [10] Giovanni Tanda and Roberto Abram. 2009. Forced convection Heat Transfer in channels with Rib Turbulators inclined at 45 deg. *Journal of Turbomachinery*, 131:021012/1-10.
- [11] Weihua Yang, Shulin Xue, Yihong He and Wei Li.2017. Experimental study on the heat transfer characteristics of high blockage ribs channel. *Experimental Thermal and Fluid Science*, 83: 248-259.
- [12] Guoliang Xu, Yang Li and Hongwu Deng. 2015. Effect of rib spacing on heat transfer and friction in a Rotating two pass square channel with asymmetrical 90 deg. Rib Turbulators. *Applied Thermal Engineering*, 80:386- 395.
- [13] Alok Chau be, Shailesh Gupta and Prakash Varma. 2014. Heat Transfer and friction factor enhancement in a square Channel having integral inclined discrete ribs on two opposite walls. *springer Journal of Mechanical Science and Technology*, 28 (5): 1927-1937.
- [14] Mohammad Ansari and Majid Bazargan.2020. Experimental and Numerical Investigation on Irregular Spacing of the Ribs in the Entry Length of a Solar Air Heater Channel. Taylor & Francis, *Science and Technology for the Built Environment*, DOI: 10.1080/23744731.2020.1793639.
- [15] Yunlin Li, Yu Rao, Keqiang Wang, Peng Zhang and Xiangyu Wub .2019. Heat Transfer and pressure loss of turbulent Flow in channels with miniature structured ribs on one wall. *International Journal of Heat and Mass Transfer*, 131:584-593.
- [16] Naveen Sharma, Andallib Tariq and Manish Sharma. 2017. Experimental investigation of heat Transfer enhancement in rectangular duct with Pentagonal Ribs. Taylor & Francis *Heat Transfer Engineering*, DOI: 10.1080/01457632.2017.1421135.
- [17] Naveen Sharma, Md Shaukat Ali, Andale Tariq and Manish Mishra.2018. Detailed heat transfer and friction factor characteristics in a rectangular duct with alternate solid and converging-slit ribs. Taylor & Francis, *Experimental Heat Transfer*, DOI: 10.1080/08916152.2018.1463306.
- [18] Safari, S.A. Abdel-Moneim and A. Bodalal. 2017. Experimental investigations of heat transfer enhancement from rectangular Duct roughened by hybrid ribs. *International Journal of Thermal Sciences*, 118: 123-138.
- [19] Kline S. J., and McClintock .1953. Describing Uncertainties in Single- Sample Experiments. *Mech. Eng. (Am. Soc. Mech. Eng.)*, 75: 3–8.